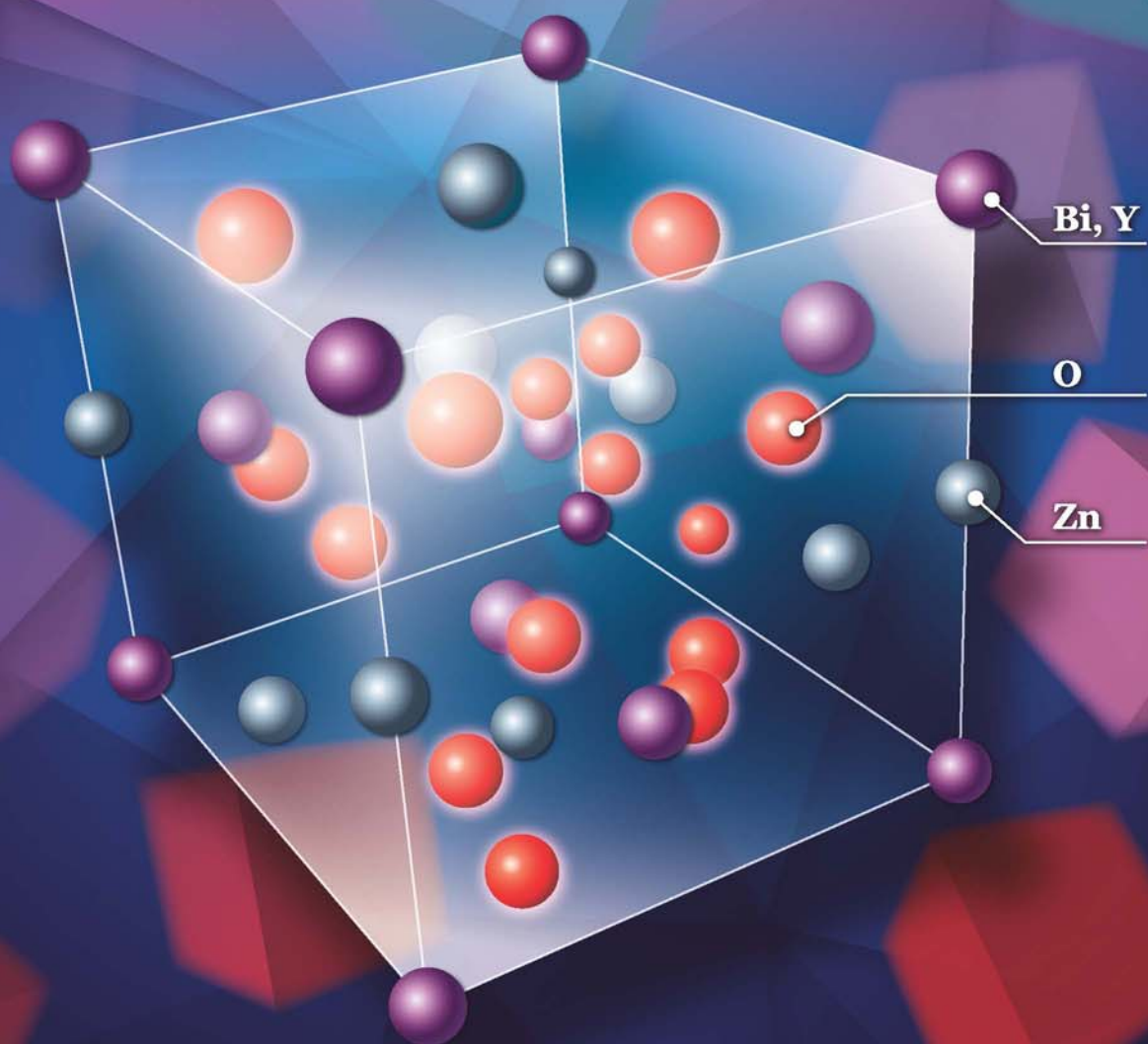


JES

JOURNAL OF
ENVIRONMENTAL
SCIENCES

March 1, 2015 Volume 29
www.jesc.ac.cn

ISSN 1001-0742
CN 11-2629/X



Sponsored by
Research Center for Eco-Environmental Sciences
Chinese Academy of Sciences

- 1 A settling curve modeling method for quantitative description of the dispersion stability of carbon nanotubes in aquatic environments
Lixia Zhou, Dunxue Zhu, Shujuan Zhang and Bingcai Pan
- 11 Antimony leaching release from brake pads: Effect of pH, temperature and organic acids
Xingyun Hu, Mengchang He and Sisi Li
- 18 Molecular diversity of arbuscular mycorrhizal fungi at a large-scale antimony mining area in southern China
Yuan Wei, Zhipeng Chen, Fengchang Wu, Hong Hou, Jining Li, Yuxian Shangguan, Juan Zhang, Fasheng Li and Qingru Zeng
- 27 Elevated CO₂ facilitates C and N accumulation in a rice paddy ecosystem
Jia Guo, Mingqian Zhang, Xiaowen Wang and Weijian Zhang
- 34 Characterization of odorous charge and photochemical reactivity of VOC emissions from a full-scale food waste treatment plant in China
Zhe Ni, Jianguo Liu, Mingying Song, Xiaowei Wang, Lianhai Ren and Xin Kong
- 45 Comparison between UV and VUV photolysis for the pre- and post-treatment of coking wastewater
Rui Xing, Zhongyuan Zheng and Donghui Wen
- 51 Synthesis, crystal structure, photodegradation kinetics and photocatalytic activity of novel photocatalyst ZnBiYO₄
Yanbing Cui and Jingfei Luan
- 62 Sources and characteristics of fine particles over the Yellow Sea and Bohai Sea using online single particle aerosol mass spectrometer
Huaiyu Fu, Mei Zheng, Caiqing Yan, Xiaoying Li, Huiwang Gao, Xiaohong Yao, Zhigang Guo and Yuanhang Zhang
- 71 Flower-, wire-, and sheet-like MnO₂-deposited diatomites: Highly efficient absorbents for the removal of Cr(VI)
Yucheng Du, Liping Wang, Jinshu Wang, Guangwei Zheng, Junshu Wu and Hongxing Dai
- 82 Methane and nitrous oxide emissions from a subtropical coastal embayment (Moreton Bay, Australia)
Ronald S. Musenze, Ursula Werner, Alistair Grinham, James Udy and Zhiguo Yuan
- 97 Insights on the solubilization products after combined alkaline and ultrasonic pre-treatment of sewage sludge
Xinbo Tian, Chong Wang, Antoine Prandota Trzcinski, Leonard Lin and Wun Jern Ng
- 106 Phosphorus recovery from biogas fermentation liquid by Ca-Mg loaded biochar
Ci Fang, Tao Zhang, Ping Li, Rongfeng Jiang, Shubiao Wu, Haiyu Nie and Yingcai Wang
- 115 Characterization of the archaeal community fouling a membrane bioreactor
Jinxue Luo, Jinsong Zhang, Xiaohui Tan, Diane McDougald, Guoqiang Zhuang, Anthony G. Fane, Staffan Kjelleberg, Yehuda Cohen and Scott A. Rice
- 124 Effect of six kinds of scale inhibitors on calcium carbonate precipitation in high salinity wastewater at high temperatures
Xiaochen Li, Baoyu Gao, Qinyan Yue, Defang Ma, Hongyan Rong, Pin Zhao and Pengyou Teng
- 131 Experimental and molecular dynamic simulation study of perfluorooctane sulfonate adsorption on soil and sediment components
Ruiming Zhang, Wei Yan and Chuanyong Jing
- 139 A fouling suppression system in submerged membrane bioreactors using dielectrophoretic forces
Alaa H. Hawari, Fei Du, Michael Baune and Jorg Thöming

(continued on inside back cover)

CONTENTS

- 146 A 1-dodecanethiol-based phase transfer protocol for the highly efficient extraction of noble metal ions from aqueous phase
Dong Chen, Penglei Cui, Hongbin Cao and Jun Yang
- 151 Intracellular biosynthesis of Au and Ag nanoparticles using ethanolic extract of *Brassica oleracea* L. and studies on their physicochemical and biological properties
Palaniselvam Kuppusamy, Solachuddin J.A. Ichwan, Narasimha Reddy Parine, Mashitah M. Yusoff, Gaanty Pragas Maniam and Natanamurugaraj Govindan
- 158 Forecasting of dissolved oxygen in the Guanting reservoir using an optimized NGBM (1,1) model
Yan An, Zhihong Zou and Yanfei Zhao
- 165 Individual particle analysis of aerosols collected at Lhasa City in the Tibetan Plateau
Bu Duo, Yunchen Zhang, Lingdong Kong, Hongbo Fu, Yunjie Hu, Jianmin Chen, Lin Li and A. Qiong
- 178 Design and demonstration of a next-generation air quality attainment assessment system for PM_{2.5} and O₃
Hua Wang, Yun Zhu, Carey Jang, Che-Jen Lin, Shuxiao Wang, Joshua S. Fu, Jian Gao, Shuang Deng, Junping Xie, Dian Ding, Xuezhen Qiu and Shicheng Long
- 189 Soil microbial response to waste potassium silicate drilling fluid
Linjun Yao, M. Anne Naeth and Allen Jobson
- 199 Enhanced catalytic complete oxidation of 1,2-dichloroethane over mesoporous transition metal-doped γ -Al₂O₃
Abbas Khaleel and Muhammad Nawaz
- 210 Role of nitric oxide in the genotoxic response to chronic microcystin-LR exposure in human-hamster hybrid cells
Xiaofei Wang, Pei Huang, Yun Liu, Hua Du, Xinan Wang, Meimei Wang, Yichen Wang, Tom K. Hei, Lijun Wu and An Xu

Available online at www.sciencedirect.com

ScienceDirect

www.journals.elsevier.com/journal-of-environmental-sciencesJOURNAL OF
ENVIRONMENTAL
SCIENCESwww.jesc.ac.cn

Experimental and molecular dynamic simulation study of perfluorooctane sulfonate adsorption on soil and sediment components

Ruiming Zhang, Wei Yan, Chuanyong Jing*

State Key Laboratory of Environmental Chemistry and Ecotoxicology, Research Center for Eco-Environmental Sciences, Chinese Academy of Sciences, Beijing 100085, China. E-mail: zhangruim07@163.com

ARTICLE INFO

Article history:

Received 30 October 2014

Revised 31 October 2014

Accepted 13 November 2014

Available online 8 January 2015

Keywords:

Humic/fulvic acid

Humin/kerogen

PFOS

Adsorption

Molecular dynamics

ABSTRACT

Soil and sediment play a crucial role in the fate and transport of perfluorooctane sulfonate (PFOS) in the environment. However, the molecular mechanisms of major soil/sediment components on PFOS adsorption remain unclear. This study experimentally isolated three major components in soil/sediment: humin/kerogen, humic/fulvic acid (HA/FA), and inorganic component after removing organics, and explored their contributions to PFOS adsorption using batch adsorption experiments and molecular dynamic simulations. The results suggest that the humin/kerogen component dominated the PFOS adsorption due to its aliphatic features where hydrophobic effect and phase transfer are the primary adsorption mechanism. Compared with the humin/kerogen, the HA/FA component contributed less to the PFOS adsorption because of its hydrophilic and polar characteristics. The electrostatic repulsion between the polar groups of HA/FA and PFOS anions was attributable to the reduced PFOS adsorption. When the soil organic matter was extracted, the inorganic component also plays a non-negligible role because PFOS molecules might form surface complexes on SiO₂ surface. The findings obtained in this study illustrate the contribution of organic matters in soils and sediments to PFOS adsorption and provided new perspective to understanding the adsorption process of PFOS on micro-interface in the environment.

© 2014 The Research Center for Eco-Environmental Sciences, Chinese Academy of Sciences.

Published by Elsevier B.V.

Introduction

Perfluorooctane sulfonate (PFOS), consisting of a sulfonate group and 8-carbon C–F tails (Appendix A Fig. S1), has been identified as an emerging contaminant of global concern (Nakayama et al., 2010; Zhang et al., 2013). Worldwide distribution and contamination of PFOS pose great threat not only to the environment, but also to the animal and human health (Beach et al., 2006; Betts, 2008; Nelson et al., 2010). PFOS can bind to peroxisome

proliferator-activated receptors which are associated with carcinogenesis, affect growth and development, and even disrupt the hormone and immune systems (Betts, 2007). Hence, a long-term and high exposure to PFOS can lead to severe symptoms such as endocrine disruption and cancer (Betts, 2007), physical development delay (Gump et al., 2011), and neonatal mortality (Kannan et al., 2010; Luebker et al., 2005).

The fate and transport of PFOS in the environment greatly depend on its adsorption on soil and sediment (Chen et al., 2012;

* Corresponding author. E-mail: cyjing@rcees.ac.cn (Chuanyong Jing).

Higgins and Luthy, 2006; Johnson et al., 2007; Ochoa-Herrera and Sierra-Alvarez, 2008). Soil and sediment are complicated matrices and generally composed of multiple complex components, which could be operationally defined as humin/kerogen, humic/fulvic acid (HA/FA), and inorganic component after chemical treatment (Mikutta et al., 2005). These components may impact PFOS adsorption with different mechanisms. However, soil and sediment are usually deemed as a single entity to investigate PFOS adsorption using kinetics and isotherm experiments (Higgins and Luthy, 2006, 2007; You et al., 2010). The lack of molecular-level knowledge of PFOS interaction with different soil/sediment components may limit our understanding and prediction of the PFOS behavior in the environment.

Molecular dynamic (MD) simulation can provide molecular level morphological and structural details on the solid–aqueous interface and has been used to study the surface adsorption and transport of pollutants. For example, MD simulation was successfully applied to study the mechanism of benzene uptake in the interlayer of montmorillonite with alkyl-methylammonium as organic substances (Zhao and Burns, 2012, 2013). Their MD results well explained the molecular mechanisms of experimental observations that the uptake capacity of organic pollutants increased with the increasing total organic content in organoclays. In our study, MD simulation was applied, as a complimentary technique to experimental observations, to investigate the role of soil/sediment components on PFOS adsorption.

The objective of our work was to explore the molecular mechanisms of PFOS adsorption on soil/sediment components. The three major components, i.e., humin/kerogen, HA/FA, and inorganic component, were isolated using extraction methods and their effects were studied with PFOS adsorption experiments. MD simulations were employed to study the interaction between PFOS and surfaces at the molecular level. Our experimental and model simulation results should improve the understanding of the solid–aqueous partition mechanisms of PFOS on environmental matrices.

1. Materials and methods

1.1. Materials

Five soil samples and one sediment sample with a wide range of total organic carbon (TOC) content (1.0%–8.3%) were collected. The soil samples were collected on the surface horizon (0–20 cm) from Liaoning Province (SY, LN), Heilongjiang Province (HL) and Beijing (BJ1, BJ2) of China, respectively. The sediment (SE) was sampled from Qinghe River in Beijing. The samples were air-dried, sieved (<2 mm) and stored at room temperature. The sample properties are given in Appendix A Table S1. Two treatment methods with NaOH and H₂O₂ were carried on to remove HA/FA and organic substances including HA/FA and humin/kerogen, respectively (Liu et al., 2008; Shi et al., 2010).

For the NaOH treatment method, HA/FA was removed, and the remaining fractions were humin/kerogen substances and inorganic component. The soil/sediment and 0.5 mol/L NaOH were mixed at a solid/solution ratio of 1:50 for at least 8 times until the solution was colorless, and each time for 6 hr (Shi et al., 2010).

For the H₂O₂ treatment method, HA/FA and humin/kerogen substances were removed, and the remaining fractions in residual were mainly inorganic component such as SiO₂ and metal oxides (Mikutta et al., 2005). Samples were mixed with 10% H₂O₂ solution at a solid/solution ratio of 1:50 for at least 3 times, each time for 6 hr (Mikutta et al., 2005). After treatment, the TOC in the treated sample was measured,

and the results are shown in Appendix A Table S1. Moreover, the TOC was consisted of 35.2%–75.9% HA/FA and 24.1%–64.8% humin/kerogen substances as shown in Appendix A Fig. S2.

1.2. Batch sorption

In kinetics experiments, an initial concentration of 200 µg/L PFOS solution in 0.01 mol/L NaCl was added to a 100 mL polypropylene bottle, adjusting with HCl and NaOH to keep the pH at 7.0 ± 0.1. At designated time intervals in a period of 7 days, a 1.5 mL sample was collected and centrifuged at 10,000 r/min for 20 min, and then PFOS in the supernatant was analyzed.

Adsorption isotherm experiments were carried out in 15 mL coming polypropylene tubes. Duplicate suspension samples contain 15 g/L of the raw/treated soil/sediment samples and 10–500 µg/L PFOS solution under the same experimental conditions to kinetics. After mixing on a rotator for 7 days, the suspension was centrifuged at 10,000 r/min for 20 min. Then, the supernatant was collected for PFOS analysis.

1.3. PFOS analysis

Dissolved PFOS concentrations were measured using an Agilent 1290 infinity liquid chromatography (Agilent Technologies, Palo Alto, CA, USA) coupled with an Agilent 6540 Ultra High Definition Q-TOF mass spectroscopy (Agilent Technologies, Santa Clara, CA, USA). Chromatographic separation was performed on an XBridge™ C-18 column (2.1 × 100 mm, 3.5 µm; Waters Corp., Dublin, Ireland) with an injection of 10 µL samples. The mobile phase consisted of 10 mmol/L ammonium acetate and acetonitrile at a molar ratio of 30:70. The operation parameters were as follows: capillary voltage 3500 V in negative; nebulizer pressure 35 psig; drying gas 10 L/min; gas temperature 350 °C; sheath gas flow 11 L/min; sheath gas temperature 250 °C; nozzle voltage 1000 V in negative ion mode; and the fragmentor voltage 60 V. The data was processed with MassHunter software (Agilent Technologies). The detection and quantification limit of PFOS were 0.3 µg/L and 1.0 µg/L, respectively. The blanks without adsorbent showed that the total PFOS loss on the centrifuge tube wall was less than 3.6% of the initial concentration. Therefore, the uptake of PFOS by solids was calculated using the mass balance.

1.4. Model rationale

In MD simulation, simple organic molecules are often used to stand for complicated natural organic matter. For example, gallic acid, protocatechuic acid, 4-hydroxybenzoic acid (Giannakopoulos et al., 2006), tetramer undecanoid acid (Aquino et al., 2011), and benzoic acid (Sun et al., 2013) have been applied to simulate humic acid and dissolved organic matter.

The organic substances in soil/sediment are consisted of various components with different structures and functional groups. In these components, HA/FA and humin/kerogen are two general constituents. HA/FA contains much polar organic carbon with polar functional groups, whereas humin/kerogen are enriched in condensed structures and lead to higher sorption affinity to nonpolar solutes (Kang and Xing, 2005; Luo et al., 2008; Wang et al., 2011). Meanwhile, humin/kerogen are more aliphatic and less polar than HA/FA because humin/kerogen contains mainly aliphatic and aromatic carbon with

less polar functional groups such as carboxyl (Kang and Xing, 2005). Based on these discrepancies in structural and polar properties, hexane and butylbenzene were chosen to represent humin/kerogen, and butylbenzoic acid with $-COOH$ group was used to emblemize HA/FA. Silicate (SiO_2) was used as a model clay mineral because it is the primary and stable composition in inorganic component (Mikutta et al., 2005). The detailed building processes of solid–aqueous layer models are provided in the Appendix A Supplementary data.

1.5. MD simulation

All molecular dynamics simulations were carried out using the Forcite module with the COMPASS force field (Sun, 1998). The water was calculated by the simple point charge model (Zhao et al., 2010). All initial solid/water interface configurations were minimized using smart minimization before running the dynamics. This stepwise scheme entails steepest-descent switching to conjugated gradient method as the energy derivatives decrease in order to accelerate the computation (Zhao et al., 2010). Equilibration and subsequent simulations were conducted in the canonical (NVT) ensemble. The system temperature was maintained at 298 K using the Andersen thermostat with an integration time step of 1.0 fs (He et al., 2013). The equations of motion were integrated using the velocity Verlet algorithm (Verlet, 1967). Initial velocities were randomly assigned according to the Boltzmann distribution (He et al., 2013), then used as the current velocity. The electrostatic interactions were calculated with the Ewald summation method (Plimpton, 1995), and the van der Waals interactions were handled by atom-based summation method with a cutoff distance of 9.5 Å (Zhao et al., 2010). Each simulation for all studied systems was preceded by a pre-equilibration period of 100 ps and followed with 2000 ps to reach equilibrium.

2. Results and discussion

2.1. Batch adsorption experiments

In the kinetics experiments, soil and sediment treated with different methods were used to represent various soil components as adsorbent for PFOS. As shown in Fig. 1, a fast uptake of PFOS from solution to solid surface was observed within the first 2 days, and the equilibrium was reached in all systems within 7 days. The kinetics could be well simulated using the pseudo second-order model, and the related parameters are listed in Appendix A Table S2.

The adsorption isotherms of PFOS are illustrated in Fig. 2 and exhibit nonlinear characters. The isotherms conform to Langmuir models for all samples. The PFOS adsorption capacity ranged 15.1–32.3 $\mu\text{g/g}$ on raw soils and sediments (Appendix A Table S3). This adsorption capacity was in consistent with previous reported values of 13.1–66.8 $\mu\text{g/g}$ on sediments (Johnson et al., 2007; You et al., 2010).

The adsorption capacity of PFOS was reduced with the decrease in TOC of treated soil/sediment samples (Fig. 2 and Appendix A Table S3), suggesting that organic substances play a key role in PFOS adsorption. Furthermore, humin/kerogen is the dominant organic substance for PFOS

adsorption on soil/sediment. For example, PFOS adsorption was reduced by 6.2%–16.4% and 29.9%–55.1%, respectively, due to the removal of HA/FA and humin/kerogen (Fig. 3). Humin/kerogen showed a higher contribution to PFOS adsorption than HA/FA because the condensed and cross-linked structures in humin/kerogen enable its higher surface hydrophobicity and larger van der Waals forces than HA/FA (Han et al., 2013; Shi et al., 2010).

Inorganic minerals, mainly silicates, were the primary constituents in soil/sediment, and attributed to 35.1%–53.6% PFOS adsorption (Fig. 3). Similarly, high (46%–66%) contributions of inorganic soil component to 1,3,5-trinitrobenzene adsorption were reported (Shi et al., 2010). In natural conditions, however, most inorganic minerals are coated with organic substances, and therefore the sorption sites on inorganic component might not be fully available (Shi et al., 2010). Thus, the contribution of inorganic component to PFOS adsorption might be overestimated in batch experimental study. Hence, the high contributions of humin/kerogen (29.9%–55.1%, Fig. 3) and HA/FA (6.2%–16.4%) may even be underestimated.

HA/FA, humin/kerogen, and inorganic component play a significant role in PFOS adsorption. However, their molecular-level interactions are still unclear. Thus, the mechanisms of PFOS uptake on different soil/sediment components were explored using MD simulation.

2.2. Equilibrium structures and density profiles by MD simulation

The effect of different components on PFOS adsorption could be evidenced by adsorption structures and density profiles, which provide information on molecular force, dynamics, and concentration distribution. The 8-PFOS loading systems were established (Appendix A Fig. S3) and their snapshots at equilibrium are shown in Fig. 4. The density profiles of PFOS along the z direction (normal to the basal surfaces) are illustrated in Fig. 5.

For SiO_2 surface, six out of 8 PFOS molecules were adsorbed on the surface, and their C–F tails and SO_3 groups could contact with the surface (Fig. 4a). The PFOS density profile exhibited in Fig. 5 showed a strong peak near zero (3.7 Å) and a weak peak at 21 Å above the SiO_2 surface. The strong peak suggested that PFOS was adsorbed on SiO_2 , consistent with batch experimental results that a range of 35.1%–53.6% PFOS was adsorbed on inorganic component. Furthermore, the structural configurations indicated that the adsorbed PFOS molecules interacted with SiO_2 surfaces by both C–F tails and SO_3 groups. This interaction may be due to hydrophobic and specific chemical adsorption for PFOS on SiO_2 (Tang et al., 2010).

For hexane modified surface, the adsorbed PFOS molecules were adjacently well-distributed on hexane modified surface (Fig. 4b), also exhibiting a strong peak at 3.7 Å and a remote peak near 47 Å (Fig. 5). The uniform distribution on hexane surface could be explained by the hydrophobic effect and the phase transfer (or absorbance) between water phase and organic phase (Hu et al., 2013; Zhao and Burns, 2012). Indeed, the aliphatic part of organic materials could play as organic phase (Higgins and Luthy, 2007). The butylbenzene modified surface also attracted PFOS close to the surface, forming a well distributed layer (Fig. 4c). It was similar to the hexane

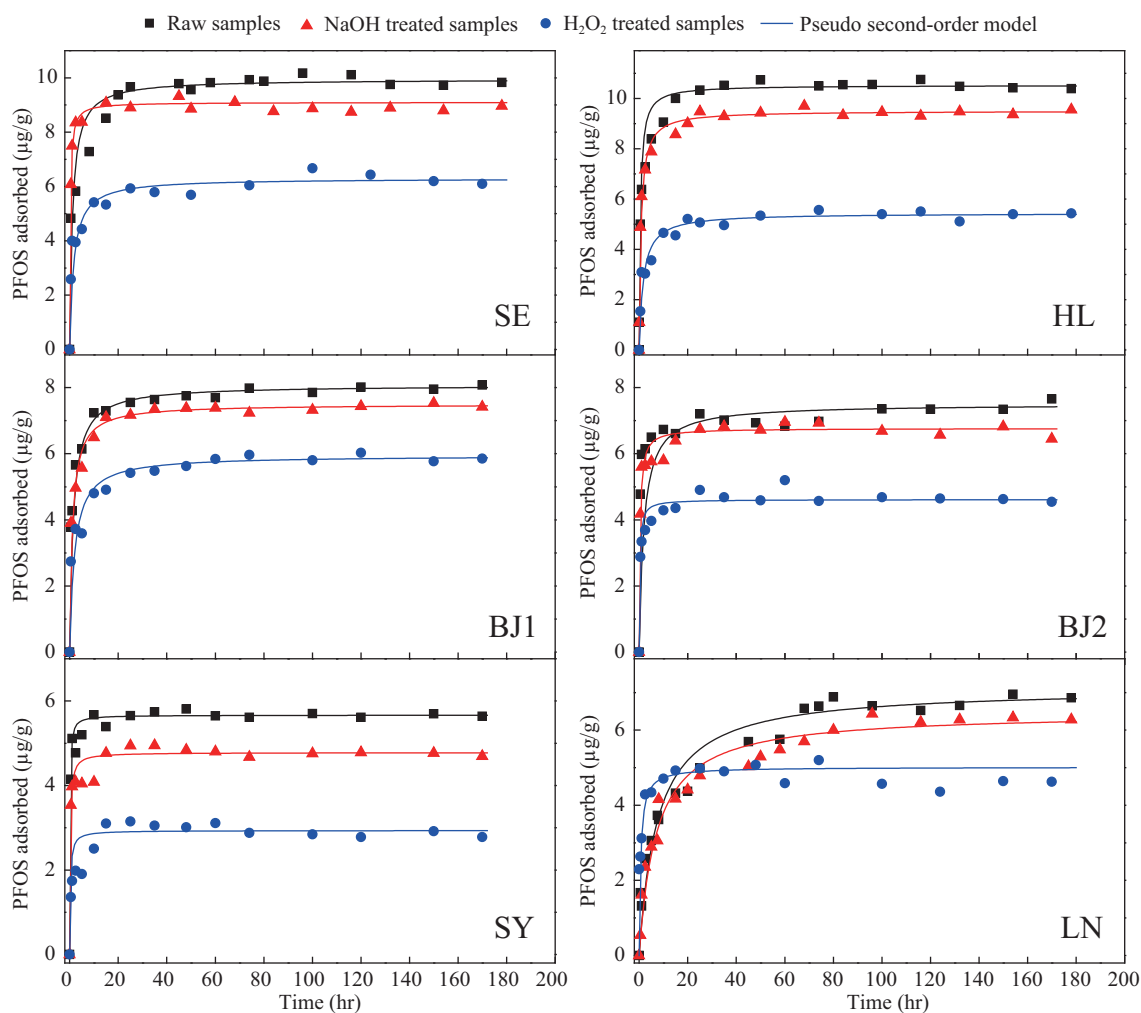


Fig. 1 – Adsorption kinetics of perfluorooctane sulfonate (PFOS) on different soil/sediment samples.

modified surface and a strongest peak near 1.8 Å was observed in Fig. 5. This phenomenon was consistent with our experimental data that humin/kerogen was as the main component contributed to PFOS adsorption (Fig. 3), suggesting the high affinity of PFOS to aliphatic and nonpolar surface.

In contrast, for butylbenzoic acid modified surface, almost no peak near the surface was observed, but a broad peak at 5–30 Å (Fig. 5). The MD results show that only one PFOS molecule was inserted into the organic layer of butylbenzoic acid modified surface (Fig. 4d); other PFOS molecules were aggregated to form micelle above the surface. This distribution indicated that PFOS is inclined to aggregate in bulk solution rather than adsorb on surface. These phenomena may be attributed to the high hydrophilic and negative charged property of carboxylic acid group on butylbenzoic acid, which repulsed the approach of both C-F tails and SO₃ groups. Considering that the HA/FA contained high hydrophilic and polar groups, the results of PFOS distribution on butylbenzoic acid modified surface agreed well with the experimental observation that HA/FA play an unimportant role on increasing PFOS adsorption on soil/sediment.

Based on the distribution structures and density profiles of PFOS on four surfaces, we concluded that PFOS adsorption benefited much more from the SiO₂ surface and hexane/butylbenzene modified surface rather than butylbenzoic modified surface. Then, the contribution of the soil/sediment components to PFOS adsorption followed the sequence: humin/kerogen ≥ inorganic component > HA/FA, which is consistent with our batch experiments (Fig. 3).

2.3. Mean squared displacement (MSD)

The average value of molecule displacement was calculated using MSD. The MSD of PFOS and H₂O molecules on various surfaces during all NVT simulated time are shown in Appendix A Fig. S4. Generally, higher mobility of the molecules could lead to a larger slope in the MSD curve. A linearity (the slope converged to 1) of the log(MSD) versus log(time) reflected that the equilibrium was achieved in our systems. The self-diffusion coefficients in Appendix A Table S4, calculated based on the Einstein relation, could be applied as index of the diffusion rate in the adsorption processes.

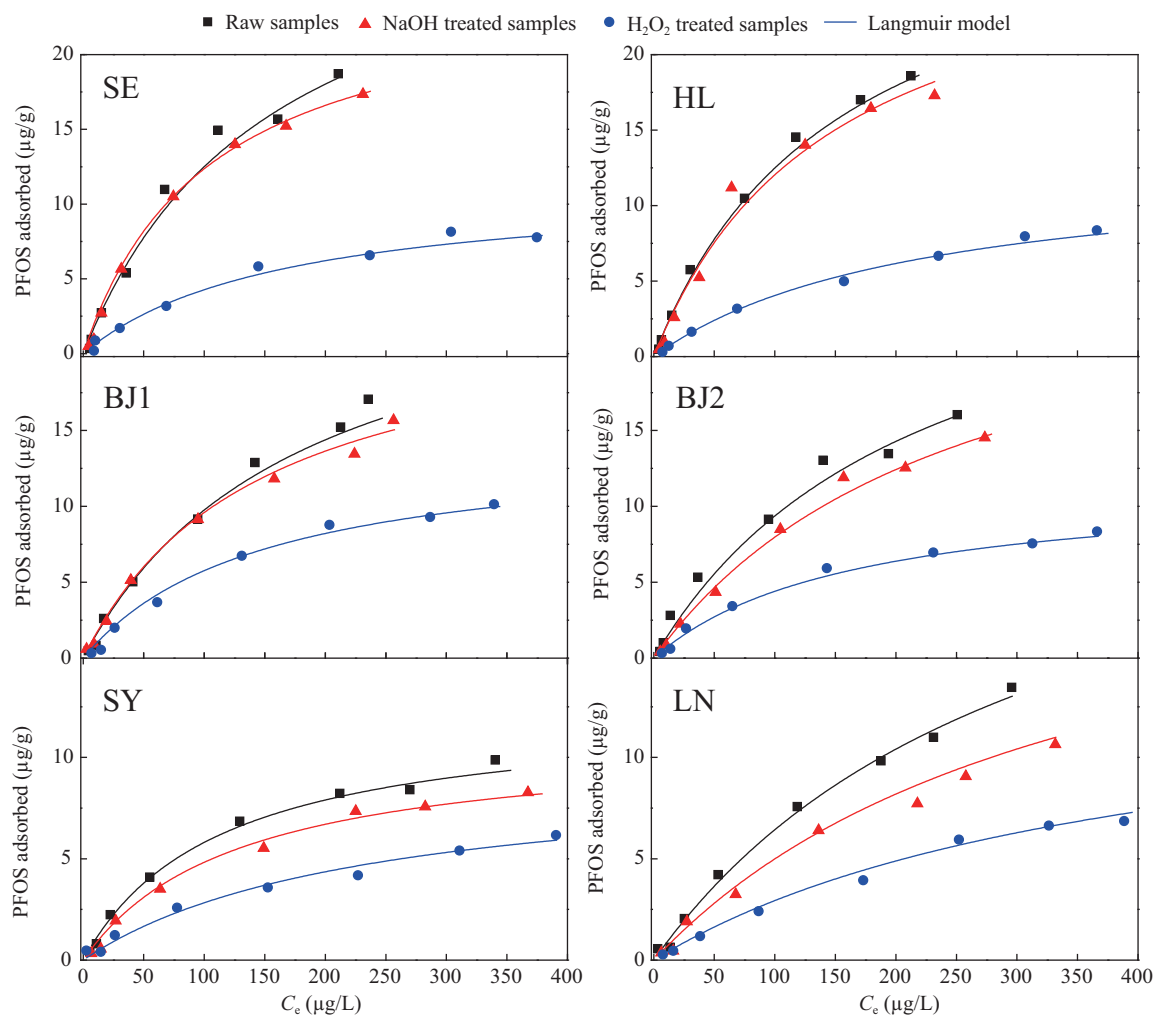


Fig. 2 – Adsorption isotherms of PFOS (perfluorooctane sulfonate) on soil/sediment samples at pH = 7, PFOS = 10–500 µg/L, adsorbents = 15 g/L.

All diffusion coefficients on four surfaces were at the order of 10^{-6} cm²/sec (Appendix A Table S4), which was in agreement with previous reported data of benzene molecules

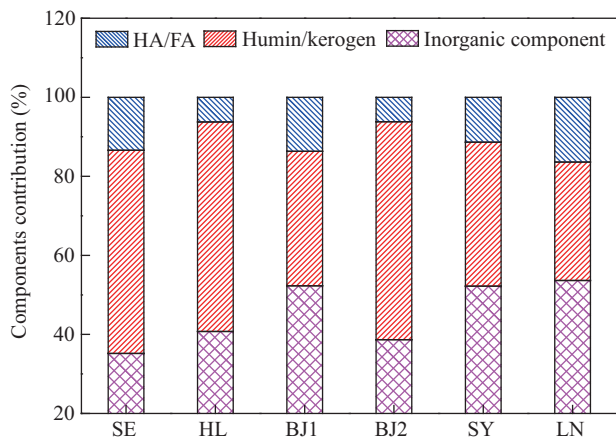


Fig. 3 – Contribution of different components (humic/fulvic acid (HA/FA), humin/kerogen, inorganic component) to PFOS adsorption on soil/sediment samples.

diffusing in the interlayers of montmorillonite with organic materials (Zhao and Burns, 2012). Furthermore, the smallest diffusion coefficient (3.1×10^{-6} cm²/sec) of PFOS occurred on hexane modified (humic/kerogen) surface. This smallest diffusion coefficient was due to the phase transformation of PFOS from water phase to hexane phase (Zhao and Burns, 2012), indicating that PFOS owns the lowest mobility and higher affinity on humin/kerogen surface (Figs. 3 and 4).

2.4. Radial distribution function

To investigate the interactions of PFOS with their surrounding molecules, radial distribution function (RDF) was calculated to provide insight into the sorption of PFOS on four surfaces. In this study, the interaction was inferred using RDF among the groups of F–F, F–H, SO₃–H, and SO₃–SO₃ between PFOS and water molecules (Fig. 6).

As shown in Fig. 6a, no obvious peak of interaction between F–F atoms from different PFOS molecules was observed on SiO₂ surface, hexane and butylbenzene modified surface. Conversely, two peaks at about 2.9 and 6.0 Å were observed on butylbenzoic acid modified surface, suggesting

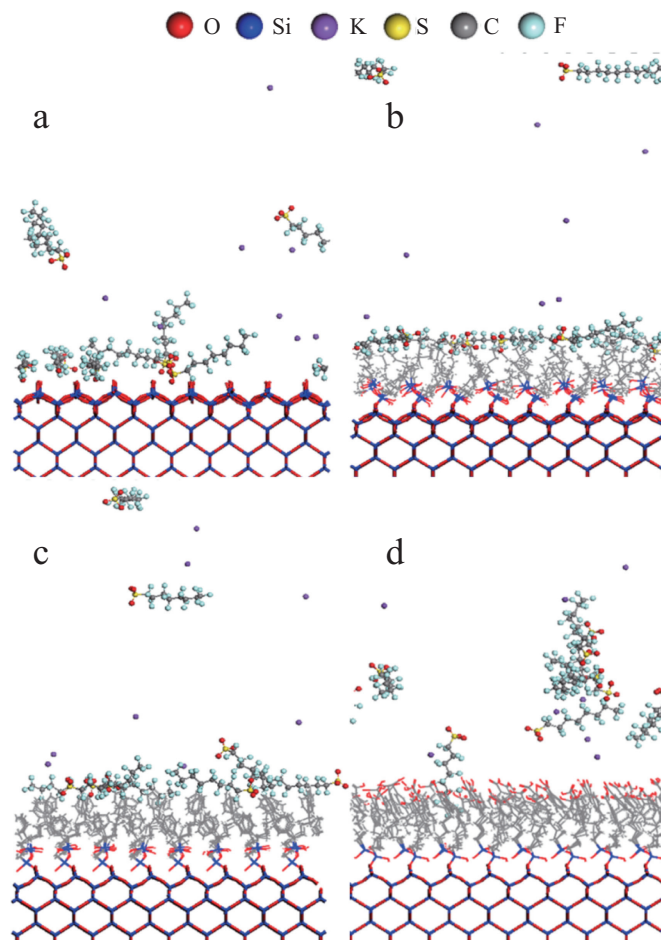


Fig. 4 – Snapshots of the simulated systems after equilibrium. (a) SiO₂ surface, (b) hexane modified, (c) butylbenzene modified, (d) butylbenzoic acid modified SiO₂ surface on side view. The water molecules were removed for visibility.

the strong F–F interaction force. Because of this F–F interaction, micelle was formed in the solution on butylbenzoic acid modified surface (Figs. 4d and 6a). Our results are in line with the finding that the perfluorinated surfactants are apt to associate with fluorinated matrices (Chen et al., 2013).

For F–H interaction, three weak peaks at 1.9, 3.7, and 6.4 Å (Fig. 6b) were observed, indicating weak interaction between PFOS molecules and water. The 1.9 Å C–F distance is within the sum of van der Waals radii of fluorine (1.47 Å) and hydrogen (1.20 Å) (Howard et al., 1996), suggesting the formation of hydrogen bond.

Similarly, a strong peak at 1.7 Å (Fig. 6c) for SO₃–H interaction indicated the existence of hydrogen bond between SO₃ group in PFOS molecules and water. In addition, the existence of SO₃–SO₃ interaction was evidenced by the broad peak around 5.0 Å (Fig. 6d).

3. Conclusions

Three major soil/sediment components including humin/kerogen, HA/FA, and inorganic component were isolated and their contributions to PFOS adsorption were investigated

using batch adsorption experiments and MD simulations. The order of the PFOS affinity on different surfaces follows humin/kerogen > inorganic component > HA/FA. Humin/kerogen dominated PFOS adsorption due to its aliphatic and nonpolar parts which facilitate phase transfer and hydrophobic

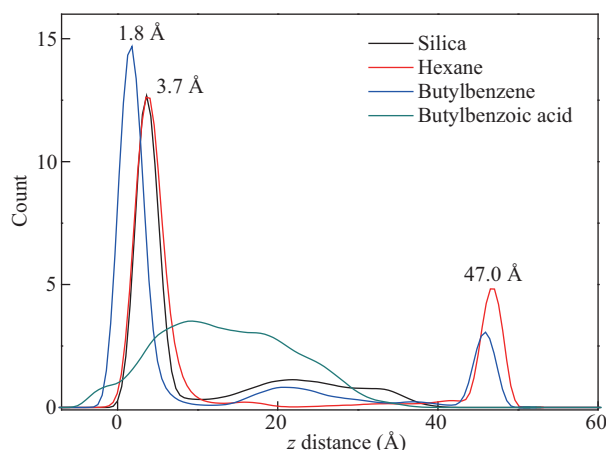


Fig. 5 – Density distributions of PFOS⁻ on SiO₂ and organic molecules modified SiO₂ surfaces.

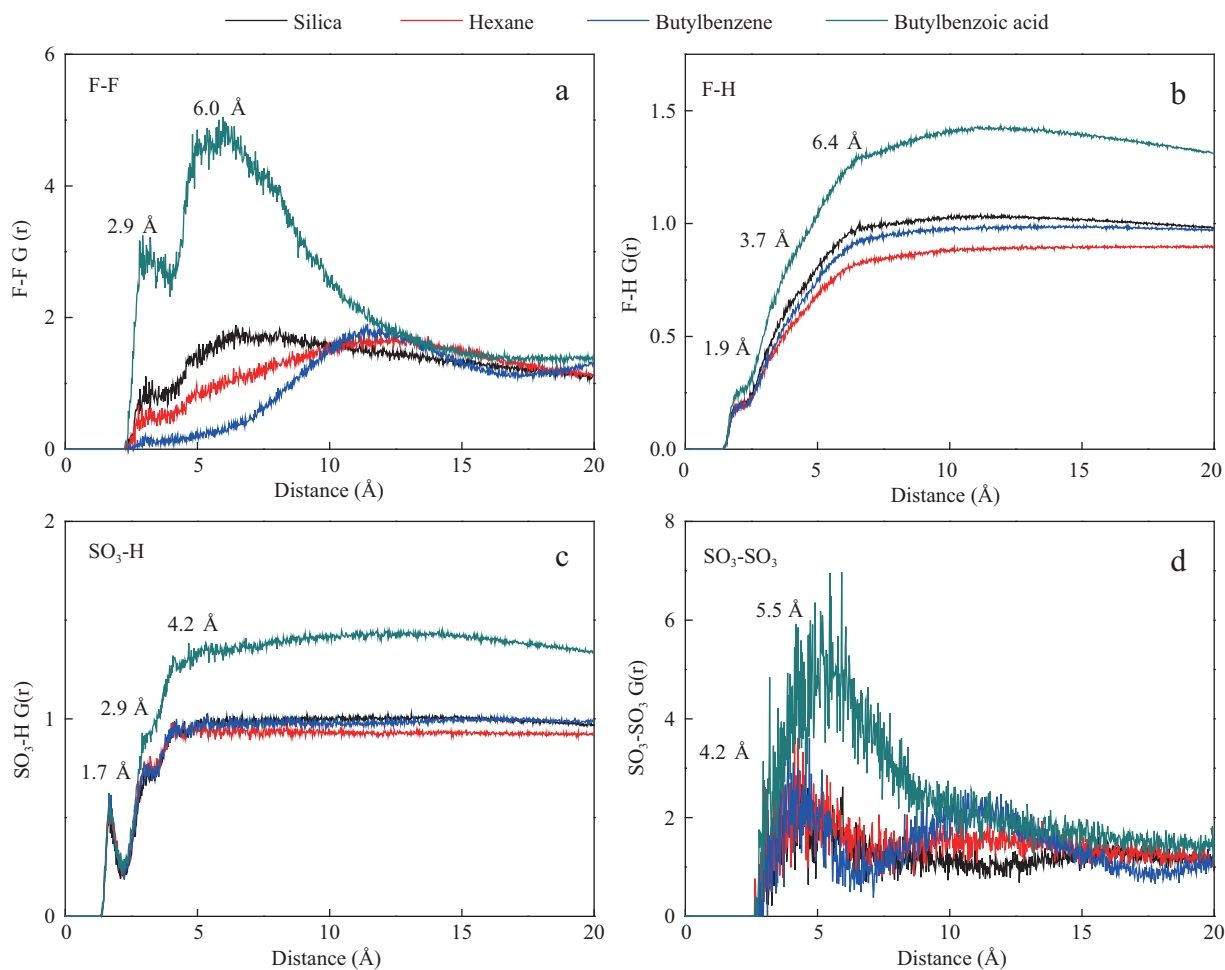


Fig. 6 – Radial distribution function (RDF) of interactions between F–F atoms (a), F–H atoms (b), SO₃–H atoms (c), and SO₃–SO₃ (d) on silica surface, hexane-modified surface, butylbenzene-modified surface, and butylbenzoic acid-modified surface.

effect. Compared with humin/kerogen, HA/FA contributed much less to PFOS adsorption because its hydrophilic and polar features may increase the electrostatic repulsion and weaken the hydrophobic effect. The inorganic component also played an important role in the PFOS adsorption, possibly due to the formation of chemical bond with surface.

The results of the present study indicate that both organic substances (especially humin/kerogen) and inorganic component were attributed to PFOS adsorption on soil and sediment. Our findings imply that PFOS adsorption mechanisms are dependent on the composition and properties of soil and sediment. Thus, a comprehensive property of organic and inorganic components should be considered to quantify the fate and transport of PFOS in the environment.

Acknowledgments

This work was supported by the National Basic Research Program (973) of China (No. 2014CB441102), the Strategic Priority Research Program of the Chinese Academy of Sciences (No. XDB14020201), and Research Center for Eco-Environmental Sciences, Chinese Academy of Sciences (No. YSW2013A01). We also thank Dr. Wei Han for providing soil samples.

Appendix A. Supplementary data

Supplementary data associated with this article can be found in online version at <http://dx.doi.org/10.1016/j.jes.2014.11.001>.

REFERENCES

- Aquino, A.J.A., Tunega, D., Pašalić, H., Schaumann, G.E., Haberhauer, G., Gerzabek, M.H., et al., 2011. Molecular dynamics simulations of water molecule-bridges in polar domains of humic acids. *Environ. Sci. Technol.* 45 (19), 8411–8419.
- Beach, S.A., Newsted, J.L., Coady, K., Giesy, J.P., 2006. Ecotoxicological evaluation of perfluorooctanesulfonate (PFOS). *Rev. Environ. Contam. Toxicol.* 186, 133–174.
- Betts, K.S., 2007. Perfluoroalkyl acids: what is the evidence telling us? *Environ. Health Perspect.* 115 (5), 250–266.
- Betts, K.S., 2008. Not immune to PFOS effects? *Environ. Health Perspect.* 116 (7), A290.
- Chen, H., Zhang, C., Yu, Y.X., Han, J.B., 2012. Sorption of perfluorooctane sulfonate (PFOS) on marine sediments. *Mar. Pollut. Bull.* 64 (5), 902–906.
- Chen, L.D., Lai, C.Z., Granda, L.P., Fierke, M.A., Mandal, D., Stein, A., et al., 2013. Fluorous membrane ion-selective electrodes for

- perfluorinated surfactants: trace level detection and in-situ monitoring of adsorption. *Anal. Chem.* 85 (15), 7471–7477.
- Giannakopoulos, E., Stathi, P., Dimos, K., Gournis, D., Sanakis, Y., Deligiannakis, Y., 2006. Adsorption and radical stabilization of humic-acid analogues and Pb^{2+} on restricted phyllosilicaceous clay. *Langmuir* 22 (16), 6863–6873.
- Gump, B.B., Wu, Q., Dumas, A.K., Kannan, K., 2011. Perfluorochemical (PFC) exposure in children: associations with impaired response inhibition. *Environ. Sci. Technol.* 45 (19), 8151–8159.
- Han, W., Luo, L., Zhang, S.Z., 2013. Adsorption of tetrabromobisphenol A on soils: contribution of soil components and influence of soil properties. *Colloids Surf. A Physicochem. Eng. Asp.* 428, 60–64.
- He, G.Z., Pan, G., Zhang, M.Y., 2013. Assembling structures and dynamics properties of perfluorooctane sulfonate (PFOS) at water-titanium oxide interfaces. *J. Colloid Interface Sci.* 405, 189–194.
- Higgins, C.P., Luthy, R.G., 2006. Sorption of perfluorinated surfactants on sediments. *Environ. Sci. Technol.* 40 (23), 7251–7256.
- Higgins, C.P., Luthy, R.G., 2007. Modeling sorption of anionic surfactants onto sediment materials: an a priori approach for perfluoroalkyl surfactants and linear alkylbenzene sulfonates. *Environ. Sci. Technol.* 41 (9), 3254–3261.
- Howard, J.A.K., Hoy, V.J., O'Hagan, D., Smith, G.T., 1996. How good is fluorine as a hydrogen bond acceptor? *Tetrahedron* 52 (38), 12613–12622.
- Hu, Y.F., Lü, W.J., Shang, Y.Z., Liu, H.L., Wang, H.L., Suh, S.H., 2013. DMSO transport across water/hexane interface by molecular dynamics simulation. *Ind. Eng. Chem. Res.* 52 (19), 6550–6558.
- Johnson, R.L., Anschutz, A.J., Smolen, J.M., Simcik, M.F., Penn, R.L., 2007. The adsorption of perfluorooctane sulfonate onto sand, clay, and iron oxide surfaces. *J. Chem. Eng. Data* 52 (4), 1165–1170.
- Kang, S.H., Xing, B.S., 2005. Phenanthrene sorption to sequentially extracted soil humic acids and humins. *Environ. Sci. Technol.* 39 (1), 134–140.
- Kannan, K., Yun, S.H., Rudd, R.J., Behr, M., 2010. High concentrations of persistent organic pollutants including PCBs, DDT, PBDEs and PFOS in little brown bats with white-nose syndrome in New York, USA. *Chemosphere* 80 (6), 613–618.
- Liu, P., Zhu, D.Q., Zhang, H., Shi, X., Sun, H.Y., Dang, F., 2008. Sorption of polar and nonpolar aromatic compounds to four surface soils of eastern China. *Environ. Pollut.* 156 (3), 1053–1060.
- Luebker, D.J., York, R.G., Hansen, K.J., Moore, J.A., Butenhoff, J.L., 2005. Neonatal mortality from in utero exposure to perfluorooctanesulfonate (PFOS) in Sprague–Dawley rats: dose–response, and biochemical and pharmacokinetic parameters. *Toxicology* 215 (1–2), 149–169.
- Luo, L., Zhang, S.Z., Ma, Y.B., 2008. Evaluation of impacts of soil fractions on phenanthrene sorption. *Chemosphere* 72 (6), 891–896.
- Mikutta, R., Kleber, M., Kaiser, K., Jahn, R., 2005. Review: organic matter removal from soils using hydrogen peroxide, sodium hypochlorite, and disodium peroxodisulfate. *Soil Sci. Soc. Am. J.* 69 (1), 120–135.
- Nakayama, S.F., Strynar, M.J., Reiner, J.L., Delinsky, A.D., Lindstrom, A.B., 2010. Determination of perfluorinated compounds in the upper Mississippi river basin. *Environ. Sci. Technol.* 44 (11), 4103–4109.
- Nelson, J.W., Hatch, E.E., Webster, T.F., 2010. Exposure to polyfluoroalkyl chemicals and cholesterol, body weight, and insulin resistance in the general US population. *Environ. Health Perspect.* 118 (2), 197–202.
- Ochoa-Herrera, V., Sierra-Alvarez, R., 2008. Removal of perfluorinated surfactants by sorption onto granular activated carbon, zeolite and sludge. *Chemosphere* 72 (10), 1588–1593.
- Plimpton, S., 1995. Fast parallel algorithms for short-range molecular dynamics. *J. Comput. Phys.* 117 (1), 1–19.
- Shi, X., Ji, L.L., Zhu, D.Q., 2010. Investigating roles of organic and inorganic soil components in sorption of polar and nonpolar aromatic compounds. *Environ. Pollut.* 158 (1), 319–324.
- Sun, H., 1998. COMPASS: an ab initio force-field optimized for condensed-phase applications overview with details on alkane and benzene compounds. *J. Phys. Chem. B* 102 (38), 7338–7364.
- Sun, Q., Xie, H.B., Chen, J.W., Li, X.H., Wang, Z., Sheng, L.X., 2013. Molecular dynamics simulations on the interactions of low molecular weight natural organic acids with C_{60} . *Chemosphere* 92 (4), 429–434.
- Tang, C.Y., Shiang Fu, Q., Gao, D., Criddle, C.S., Leckie, J.O., 2010. Effect of solution chemistry on the adsorption of perfluorooctane sulfonate onto mineral surfaces. *Water Res.* 44 (8), 2654–2662.
- Verlet, L., 1967. Computer “Experiments” on classical fluids. I. Thermodynamical properties of Lennard–Jones molecules. *Phys. Rev.* 159 (1), 98–103.
- Wang, X.L., Guo, X.Y., Yang, Y., Tao, S., Xing, B.S., 2011. Sorption mechanisms of phenanthrene, lindane, and atrazine with various humic acid fractions from a single soil sample. *Environ. Sci. Technol.* 45 (6), 2124–2130.
- You, C., Jia, C.X., Pan, G., 2010. Effect of salinity and sediment characteristics on the sorption and desorption of perfluorooctane sulfonate at sediment–water interface. *Environ. Pollut.* 158 (5), 1343–1347.
- Zhang, K.L., Huang, J., Yu, G., Zhang, Q.W., Deng, S.B., Wang, B., 2013. Destruction of perfluorooctane sulfonate (PFOS) and perfluorooctanoic acid (PFOA) by ball milling. *Environ. Sci. Technol.* 47 (12), 6471–6477.
- Zhao, Q., Burns, S.E., 2012. Molecular dynamics simulation of secondary sorption behavior of montmorillonite modified by single chain quaternary ammonium cations. *Environ. Sci. Technol.* 46 (7), 3999–4007.
- Zhao, Q., Burns, S.E., 2013. Modeling sorption and diffusion of organic sorbate in hexadecyltrimethylammonium-modified clay nanopores—a molecular dynamics simulation study. *Environ. Sci. Technol.* 47 (6), 2769–2776.
- Zhao, T.T., Xu, G.Y., Yuan, S.L., Chen, Y.J., Yan, H., 2010. Molecular dynamics study of alkyl benzene sulfonate at air/water interface: effect of inorganic salts. *J. Phys. Chem. B* 114 (15), 5025–5033.



Editorial Board of Journal of Environmental Sciences

Editor-in-Chief

X. Chris Le University of Alberta, Canada

Associate Editors-in-Chief

Jiuhui Qu Research Center for Eco-Environmental Sciences, Chinese Academy of Sciences, China
Shu Tao Peking University, China
Nigel Bell Imperial College London, UK
Po-Keung Wong The Chinese University of Hong Kong, Hong Kong, China

Editorial Board

Aquatic environment

Baoyu Gao
Shandong University, China
Maohong Fan
University of Wyoming, USA
Chihpin Huang
National Chiao Tung University
Taiwan, China
Ng Wun Jern
Nanyang Environment &
Water Research Institute, Singapore
Clark C. K. Liu
University of Hawaii at Manoa, USA
Hokyong Shon
University of Technology, Sydney, Australia
Zijian Wang
Research Center for Eco-Environmental Sciences,
Chinese Academy of Sciences, China
Zhiwu Wang
The Ohio State University, USA
Yuxiang Wang
Queen's University, Canada
Min Yang
Research Center for Eco-Environmental Sciences,
Chinese Academy of Sciences, China
Zhifeng Yang
Beijing Normal University, China
Han-Qing Yu
University of Science & Technology of China,
China

Terrestrial environment

Christopher Anderson
Massey University, New Zealand
Zucong Cai
Nanjing Normal University, China
Xinbin Feng
Institute of Geochemistry,
Chinese Academy of Sciences, China
Hongqing Hu
Huazhong Agricultural University, China
Kin-Che Lam
The Chinese University of Hong Kong
Hong Kong, China
Erwin Klumpp
Research Centre Juelich, Agrosphere Institute
Germany

Peijun Li

Institute of Applied Ecology,
Chinese Academy of Sciences, China
Michael Schloter
German Research Center for Environmental Health
Germany
Xuejun Wang
Peking University, China
Lizhong Zhu
Zhejiang University, China

Atmospheric environment

Jianmin Chen
Fudan University, China
Abdelwahid Mellouki
Centre National de la Recherche Scientifique
France
Yujing Mu
Research Center for Eco-Environmental Sciences,
Chinese Academy of Sciences, China
Min Shao
Peking University, China
James Jay Schauer
University of Wisconsin-Madison, USA
Yuesi Wang
Institute of Atmospheric Physics,
Chinese Academy of Sciences, China
Xin Yang
University of Cambridge, UK

Environmental biology

Yong Cai
Florida International University, USA
Henner Hollert
RWTH Aachen University, Germany
Jaeseong Lee
Sungkyunkwan University, South Korea
Christopher Rensing
University of Copenhagen, Denmark
Bojan Sedmak
National Institute of Biology, Slovenia
Lirong Song
Institute of Hydrobiology,
Chinese Academy of Sciences, China
Chunxia Wang
National Natural Science Foundation of China
Gehong Wei
Northwest A & F University, China

Daqiang Yin

Tongji University, China
Zhongtang Yu
The Ohio State University, USA

Environmental toxicology and health

Jingwen Chen
Dalian University of Technology, China
Jianning Hu
Peking University, China
Guibin Jiang
Research Center for Eco-Environmental Sciences,
Chinese Academy of Sciences, China
Sijin Liu
Research Center for Eco-Environmental Sciences,
Chinese Academy of Sciences, China
Tsuyoshi Nakanishi
Gifu Pharmaceutical University, Japan
Willie Peijnenburg
University of Leiden, The Netherlands
Bingsheng Zhou
Institute of Hydrobiology,
Chinese Academy of Sciences, China

Environmental catalysis and materials

Hong He
Research Center for Eco-Environmental Sciences,
Chinese Academy of Sciences, China
Junhua Li
Tsinghua University, China
Wenfeng Shangguan
Shanghai Jiao Tong University, China
Ralph T. Yang
University of Michigan, USA

Environmental analysis and method

Zongwei Cai
Hong Kong Baptist University,
Hong Kong, China
Jiping Chen
Dalian Institute of Chemical Physics,
Chinese Academy of Sciences, China
Minghui Zheng
Research Center for Eco-Environmental Sciences,
Chinese Academy of Sciences, China
Municipal solid waste and green chemistry
Pinjing He
Tongji University, China

Editorial office staff

Managing editor Qingcai Feng
Editors Zixuan Wang Suqin Liu Kuo Liu Zhengang Mao
English editor Catherine Rice (USA)

JOURNAL OF ENVIRONMENTAL SCIENCES

环境科学学报(英文版)

www.jesc.ac.cn

Aims and scope

Journal of Environmental Sciences is an international academic journal supervised by Research Center for Eco-Environmental Sciences, Chinese Academy of Sciences. The journal publishes original, peer-reviewed innovative research and valuable findings in environmental sciences. The types of articles published are research article, critical review, rapid communications, and special issues.

The scope of the journal embraces the treatment processes for natural groundwater, municipal, agricultural and industrial water and wastewaters; physical and chemical methods for limitation of pollutants emission into the atmospheric environment; chemical and biological and phytoremediation of contaminated soil; fate and transport of pollutants in environments; toxicological effects of terrorist chemical release on the natural environment and human health; development of environmental catalysts and materials.

For subscription to electronic edition

Elsevier is responsible for subscription of the journal. Please subscribe to the journal via <http://www.elsevier.com/locate/jes>.

For subscription to print edition

China: Please contact the customer service, Science Press, 16 Donghuangchenggen North Street, Beijing 100717, China. Tel: +86-10-64017032; E-mail: journal@mail.sciencep.com, or the local post office throughout China (domestic postcode: 2-580).

Outside China: Please order the journal from the Elsevier Customer Service Department at the Regional Sales Office nearest you.

Submission declaration

Submission of the work described has not been published previously (except in the form of an abstract or as part of a published lecture or academic thesis), that it is not under consideration for publication elsewhere. The publication should be approved by all authors and tacitly or explicitly by the responsible authorities where the work was carried out. If the manuscript accepted, it will not be published elsewhere in the same form, in English or in any other language, including electronically without the written consent of the copyright-holder.

Editorial

Authors should submit manuscript online at <http://www.jesc.ac.cn>. In case of queries, please contact editorial office, Tel: +86-10-62920553, E-mail: jesc@rcees.ac.cn. Instruction to authors is available at <http://www.jesc.ac.cn>.

Journal of Environmental Sciences (Established in 1989) Volume 29 2015

Supervised by	Chinese Academy of Sciences	Published by	Science Press, Beijing, China
Sponsored by	Research Center for Eco-Environmental Sciences, Chinese Academy of Sciences		Elsevier Limited, The Netherlands
Edited by	Editorial Office of Journal of Environmental Sciences P. O. Box 2871, Beijing 100085, China Tel: 86-10-62920553; http://www.jesc.ac.cn E-mail: jesc@rcees.ac.cn	Distributed by	Domestic Science Press, 16 Donghuangchenggen North Street, Beijing 100717, China Local Post Offices through China Foreign Elsevier Limited http://www.elsevier.com/locate/jes
Editor-in-chief	X. Chris Le	Printed by	Beijing Beilin Printing House, 100083, China

CN 11-2629/X

Domestic postcode: 2-580

Domestic price per issue RMB ¥ 110.00

ISSN 1001-0742

